ELSEVIER

Polymer Degradation and Stability 79 (2003) 111–121

Polymer Degradation and Stability

www.elsevier.com/locate/polydegstab

Processing degradation of polyamide 6/montmorillonite clay nanocomposites and clay organic modifier

Rick D. Davis[a,*], Jeffery W. Gilman[a,1], David L. VanderHart[b,2]

[a]*Building and Fire Research Laboratory, National Institute of Standards and Technology, 100 Bureau Drive, Gaithersburg, MD 20899-8665, USA*
[b]*Polymers Division, National Institute of Standards and Technology, 100 Bureau Drive, Gaithersburg, MD 20899-8544, USA*

Received 23 May 2002; received in revised form 6 August 2002; accepted 6 August 2002

Abstract

Under injection molding conditions, typical of industrial processing, in situ polymerized montmorillonite/polyamide 6 nanocomposites significantly degraded, producing a four-fold increase in ε-caprolactam (monomer) content and a significant reduction in number average molecular mass, as compared to the as-received nanocomposite. Degradation was believed to occur via peptide bond scission following attack by water that is most likely released from the polymer and the montmorillonite clay surface at the 300 °C (12.5 min) processing conditions. Under identical injection molding conditions, virgin polyamide 6 number average molecular mass did not decrease (within experimental uncertainty); however, a small increase in monomer content was observed. Characterization methods included solution ^{13}C nuclear magnetic resonance spectroscopy, infrared spectroscopy, gel-permeation chromatography, and thermal gravimetric analysis.

Keywords: Polyamide 6; Nanocomposite; Montmorillonite clay; Thermal degradation; Processing stability; Nuclear magnetic resonance spectroscopy

1. Introduction

The main motivations for studying polymer clay nanocomposites containing micron sized nanometer thin aluminosilicate sheets dispersed in a polymer matrix are associated with improved heat distortion temperature [1] and barrier properties, increased modulus [2], and reduced flammability of polymers containing just a few % mass fraction of clay [3]. The success of these materials requires that the incorporation of the organically modified clay has negligible adverse affects on preparation, cost, processing stability, and a host of other application-specific performance properties. Previous work in our laboratory preliminarily addressed some of the processing issues associated with nanocomposites [4]. We found that during melt blending MMT/PA-6 nanocomposites in a twin-screw extruder at 240 °C, a particular quaternary alkyl ammonium treatment on the montmorillonite clay (MMT) degraded to an extent correlated with extruder residence times. Also, for in situ polymerized nanocomposites, which were injection molded at 295 °C, an irreversible change occurred such that the normal γ-phase of the PA-6 crystallites was more extensively converted to the α-phase upon annealing at 214 °C. After subsequent processing the nanocomposites by injection molding at 295 °C, we observed irreversible partial transformation of γ to α crystallites. This permanent instability of the γ structure we proposed to result from thermal degradation of the organic modifier and/or degradation of the PA-6 polymer during processing at 295 °C and in the presence of MMT. To explore these possibilities we undertook a study of in situ MMT/PA-6 nanocomposite thermal stability during processing at 300 °C and sought to determine if there was degradation of PA-6.

* Corresponding author. Tel.: +1-301-975-6698; fax: +1-301-975-4052.

E-mail addresses: rick.davis@nist.gov (R.D. Davis), jeffrey.gilman@nist.gov (J.W. Gilman), david.vanderhart@nist.gov (D.L. VanderHart).

[1] Tel.: +1-301-975-6573; fax: +1-301-975-4052.

[2] Tel.: +1-301-975-6754; fax: +1-301-975-3928.

0141-3910/02/$ - see front matter © 2002 Elsevier Science Ltd. All rights reserved.
PII: S0141-3910(02)00263-X

2. Background

Numerous polyamide 6 (PA-6) thermal degradation products (small molecules and polymer end-groups) have been identified [5–8]. Their amount and nature are strongly dependent on the environment; i.e. temperature and the presence of a nucleophile (Fig. 1). The major PA-6 thermal decomposition products can be separated into three categories: (1) those generated at temperatures below 300 °C in the absence of a nucleophile (Fig. 1A), (2) those generated at temperatures much greater than 300 °C in the absence of a nucleophile (Fig. 1A), and (3) those that form in the presence of a nucleophile, specifically water (Fig. 1B).

The following discussion summarizing PA-6 thermal decomposition is based on a review by Levchik [5] and references found within, unless otherwise specifically referenced.

(1) Below 300 °C and in the absence of a nucleophile, PA-6 thermal degradation occurs primarily via ε-caprolactam (monomer) formation (Fig. 2). Monomer formation often begins at temperatures slightly above 200 °C and primarily occurs by intramolecular end-group cyclization (end-biting, Fig. 2A and B) and cyclization within the polymer main chain (back-biting, Fig. 2C). Monomer formation occurs, but to a lesser degree via intermolecular aminolysis and acidolysis between two polymer chains (Fig. 2D). A loss of a few percent of monomer via these intramolecular mechanisms is typical. A few percent mass loss is within the experimental uncertainty of most conventional molecular mass characterization techniques; therefore, degradation via these routes often is difficult to detect by measuring PA-6 molecular mass.

Larger cyclic units are also products of PA-6 thermal degradation. Luderwald et al. [9] reported that cyclic

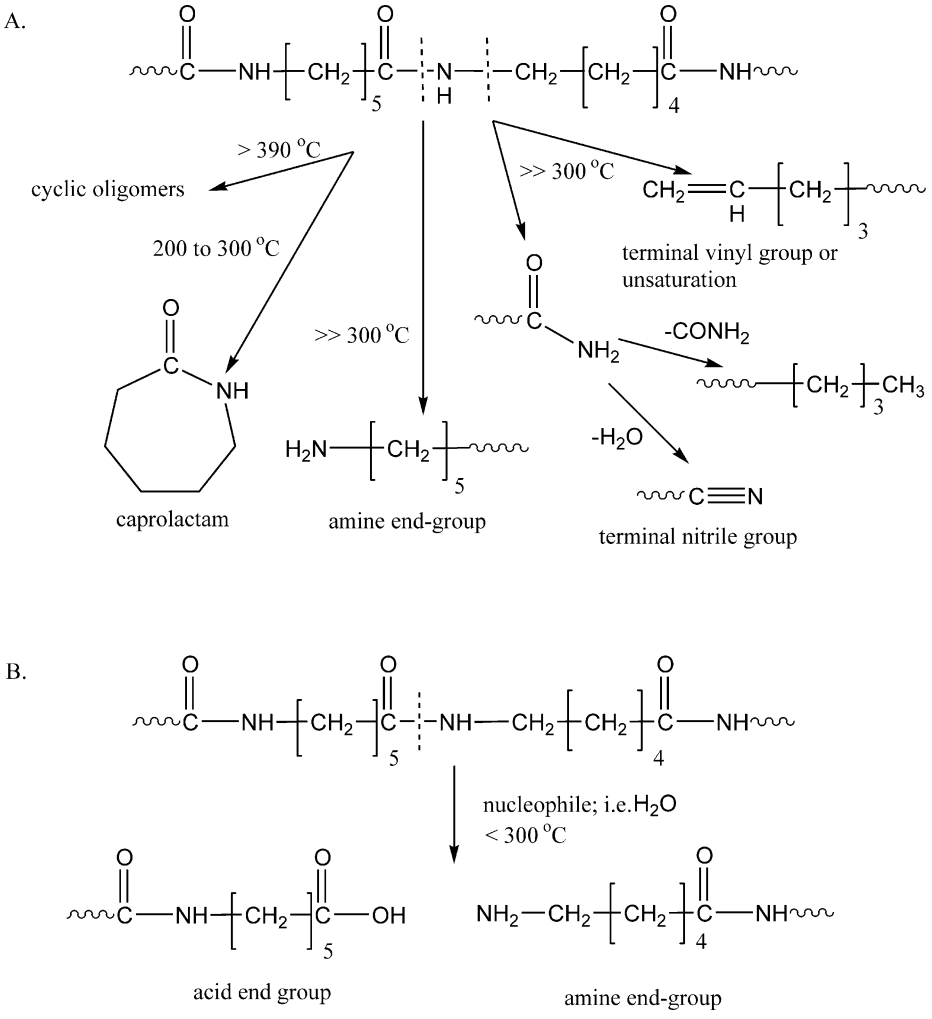

Fig. 1. Dominant PA-6 thermal degradation products in the absence of a nucleophile (A) and in the presence of a nucleophile, such as water (B). Our PA-6 materials were processed at 300 °C and presumably only experience degradation via caprolactam formation or nucleophilic attack, unless clay catalyzes one of the other degradation routes.

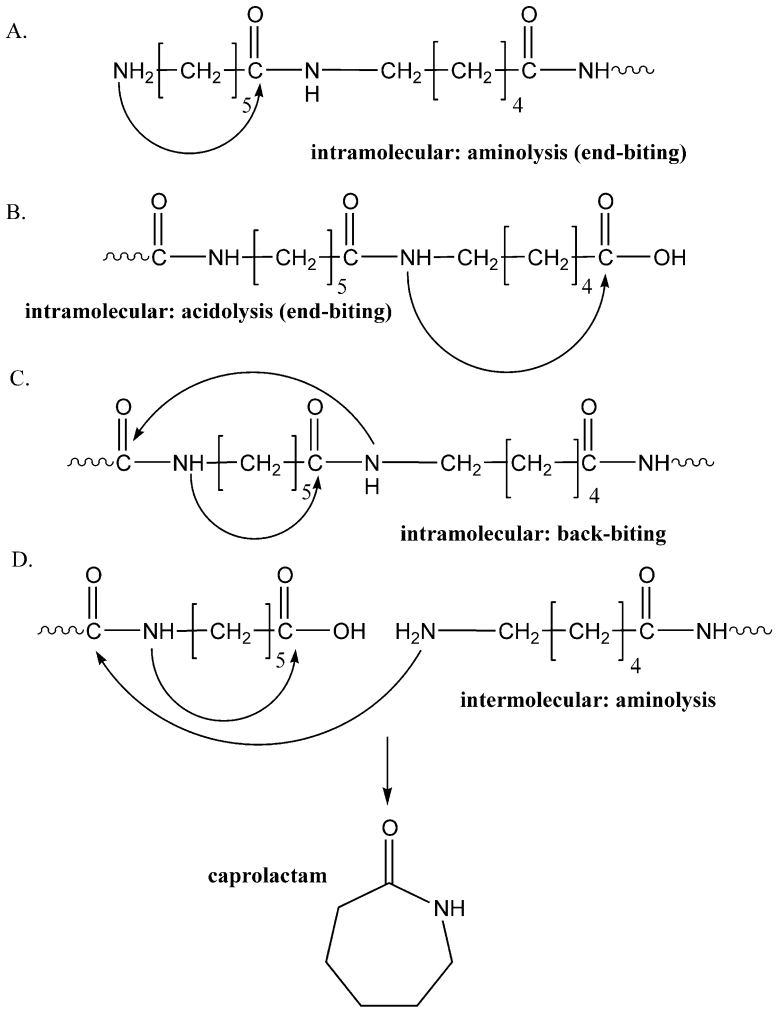

Fig. 2. Illustrated are the intra- and intermolecular routes that generate ε-caprolactam and larger cyclics. For simplicity, only monomer formation is shown. The arrows do not represent electron-pushing mechanisms rather, they connect those pairs of atoms that form new bonds. Studies have shown that a vast majority of cyclics are formed via intramolecular pathways and that the formation of monomer is observed above 200 °C, whereas larger cyclics are generated at temperatures greater than 390 °C.

oligomers (cyclic moieties consisting of multiple polymer repeat units) are generated as thermal decomposition products of PA-6 at temperatures above 390 °C and Ballisteri et al. [10] suggested that the mechanism for cyclic formation is via intramolecular and intermolecular aminolysis (Fig. 2A and D).

(2) In most cases, the higher than 300 °C products are observed at temperatures ranging from 500 to 800 °C. At these elevated temperatures and in the absence of a nucleophile, PA-6 thermal degradation results in the formation of monomer, cyclic oligomers, various small gaseous molecules and polymer chain end-groups whose compositions are each indicative of the site and mode of degradation (Fig. 1). As an example, scission of the thermally weakest bond, the alkyl–amide linkage bond ($NH–CH_2$), results in the formation of a terminal unsaturation and an amide group; the latter immediately decomposes to a terminal nitrile or methyl group. Unlike the monomer-forming mechanisms discussed above and shown in Fig. 2, these higher temperature degradation routes shown in Fig. 1 result from catastrophic thermal degradation of PA-6.

(3) In the presence of a nucleophile such as water, or an additive such as ammonium polyphosphate [8,11], the decomposition thermodynamics of PA-6 are altered. For example, the weakest links are: hydrolysis of peptide linkages near 300 °C (Fig. 1B), and thermal homolytic scission of alkyl-amide bonds at temperature greater than 500 °C (Fig. 1A). Hydrolytic peptide scission results in a drastic decrease in polymer molecular mass and an increase in polymer end-groups content. Thus, the presence of water leads to an increase in monomer formation and an increase in polymer end-group concentration.

Table 1
Description and sample identification names of PA-6 and nanoPA-6 polymers

Sample ID	Description
PA-6-e	As received, extruded PA-6 pellets
PA-6-i	80 °C dried then 300 °C injection molded PA-6-e
PA-6-i2	120 °C dried then 300 °C injection molded PA-6-e
MMT/PA-6-e	As received, *in situ* polymerized then extruded 1-lauric acid-12-tertiary ammonium treated montmorillonite/PA-6 nanocomposite pellets
MMT/PA-6-i	80 °C dried then 300 °C injection molded MMT/PA-6-e
MMT/PA-6-i2	120 °C dried then 300 °C injection molded MMT/PA-6-e

All drying times are 4 h.

3. Experimental[3,4]

Table 1 lists the descriptions and sample identification names of PA-6 and nanoPA-6 polymers investigated in this study. For the remainder of this publication the name "nanoPA-6″ will refer to all MMT/PA-6 nanocomposites involved in this study and the sample identification names (provided in Table 1) will refer to a specific MMT/PA-6, which has been exposed to particular drying temperatures and processing conditions.

Virgin PA-6 and MMT/PA-6 pellets (PA-6-e and MMT/PA-6-e) were provided by a commercial source [12]. MMT/PA-6-e was synthesized via in situ polymerization in the presence of 5% mass fraction of MMT[5] that was treated with the ammonium salt of 12-aminolauric acid. The nanoPA-6 TEM revealed that the nanocomposites were highly exfoliated.

The PA-6 pellets were stored at ambient conditions until processing. Immediately prior to injection molding, the pellets were dried for 4 h either at 80 °C or 120 °C in a convection oven [13]. Samples were then cooled to room temperature in the oven, and stored in a nitrogen atmosphere. Injection molding employed a GLUCO LP20B semiautomatic press operating at a 0.36 MN (20 ton) clamping force at 0.69 M*p*a (100 psi) air pressure. Typically, the PA-6 pellets were placed in the melting chamber for a 12.5 min residence time at 300 °C in an argon atmosphere. In order to facilitate even heating and complete melting within the melting chamber, a four-channel spreader was used to divide the molten polymer into these four channels, thus creating more polymer to metal surface contact. The molten polymer was injected into a mold held at 80 °C and in an argon atmosphere. The 75 mm round, 8 mm thick processed samples were removed from the mold after 4 min, and then were stored in ambient conditions.

Solution ^{13}C NMR spectra were collected on a Bruker Avance 300 MHz NMR operating at a spectral frequency of 75.48 MHz for carbon. A routine single pulse ^{13}C pulse program was employed with a 20 μs 90° carbon pulse, 3 s recycle delay, and broadband proton decoupling. A 10 mm multinuclear NMR probe was used with the average number of transients being 30,000 (~36 h) to give sufficient signal-to-noise to allow quantitation of end-groups and residual monomer.

Solution ^{13}C NMR samples were prepared by dissolving PA-6 and PA-6 nanocomposites in 2,2,2-trifluoroethanol (TFE) with gentle heating, then adding deuterochloroform ($CDCl_3$) to the cooled solution to give a sample with about 5% mass fraction polymer in a solvent consisting of 80:20 TFE to $CDCl_3$; solvent pH value was 5.4 but will be referred to as neutral [14]. Basic solvent NMR samples were prepared in a similar manner, however 25% of the TFE was the potassium salt of TFE; at a pH value of ~11; therefore, the ratio of TFE:TFE^-K^+:$CDCl_3$ is 60:20:20.

Polymer composition values are provided in Table 2 and were calculated based on integrals of PA-6 carbons associated with amine and acid end-group peaks (α_{NH2} and α_{CO2H} or α_{CO2-}) ratioed to a PA-6 polymer backbone integral, typically the CH_2 labeled as "1″. Residual monomer contents were similarly determined using the 1_m or $2'_m$ peaks (nomenclature is defined in Fig. 3). PA-6 number average molecular masses[6] were calculated using Eq. (1).

$$M_n = [(1 + 1_{cis}) \times 113.16\ \text{g/mol}]/[0.5 \times (\alpha_{NH2} + \alpha_{CO2H})] \quad (1)$$

[3] Certain commercial equipment, instruments, materials, services, or companies are identified in this paper in order to specify adequately the experimental procedure. This in no way implies endorsement or recommendation by NIST. In addition, NIST is not liable for the accuracy of the results from experiments not conducted at NIST.

[4] The policy of the National Institute of Standards and Technology (NIST) is to use metric units of measurement in all its publications, and to provide statements of uncertainty for all original measurements. In this document however, data from organizations outside NIST are shown, which may include measurements in non-metric units or measurements without uncertainty statements.

[5] Most MMT is paramagnetic resulting mainly from embedded Fe^{3+} that occupies a portion of the Al^{3+} octahedral sites located in the central layer of the 3 layer sandwich that constitutes a single clay sheet; the outer layers are silicon oxide tetrahedrals.

[6] According to ISO 31-8, the term "molecular mass" has been replaced by "relative molecular mass", symbol M_r. Thus, if this nomenclature and notation were used here, $M_{r,n}$ instead of the historically conventional M_n for the average molecular mass (with similar notation for M_w, M_z, M_v) would be used. It could be called the "number average relative molecular mass". The conventional notation, rather than the ISO notation, has been employed here.

Table 2
Composition data from solution ^{13}C NMR analysis of virgin PA-6 and nanoPA-6 pellets and 300 °C processed

Polymer	M_n (g/mol)[b]	ε- Caprolactam[a]	End-groups[a]		
			Amine	Acid	% Δ
PA-6-e	13620±1450	0.00	0.0083	0.0083	0
PA-6-i	12310±1490	0.0092	0.0092	0.0092	0
MMT/PA-6-e	13670±1500	0.0019	0.0083	0.0083	0
MMT/PA-6-i	7490±630	0.0038	0.0083	0.0151	53
MMT/PA-6-i2	8380±1490	0.0048	<0.001	0.0135	>70

Composition contents are expressed as fractions of monomer and monomer repeat units with polymer end-groups relative to the total number of monomer units. -i and -e = 80 °C drying before injection molding. -i2 = 120 °C drying before injection molding.

[a] Experimental uncertainty: ±5% of the value, except for MMT/PA-6-i2 (±10%).

[b] Experimental uncertainty: ~±10% of the value, except for MMT/PA-6-i2 (±20%).

where 1, 1_{cis}, α_{NH2}, and α_{CO2H} or α_{CO2-} represent the integrals of NMR peaks as defined in Fig. 3 and 113.16 g/mol is the repeat unit molecular mass. Integrals were measured 3–5 times using XWIN-NMR software (average values used for calculations). The standard uncertainty (1σ) in molecular mass is ±10% of the value, except for MMT/PA-6-i2, which was ±20%. Uncertainties related to the quantitation of end-groups and residual monomer is ±5% of the value, except for MMT/PA-6-i2, which was ±10%; these were based on the repeatability of the integrals. The larger uncertainty in MMT/PA-6-i2 values stems from a lower signal-to-noise spectrum, and therefore the less reproducible integration of acid end-group peaks and monomer peaks. Amine end-group peaks were not distinguishable from the noise indicating that within experimental uncertainty amine end-group fraction is less than 0.001.

Integration of (small) end-group peaks was performed by overlaying a spectrum onto itself, then reducing the intensity and altering the peak width of a larger isolated peak in one spectrum until its shape and size match that of a smaller peak of interest in the other spectrum. The spectra were horizontally shifted, subtracted from each other, and then adjustments in the larger peak's intensity were again made until there was no distinguishable peak at the smaller peak location in the difference spectrum. Using XWIN-NMR software, this technique produces a scaling factor, which, when multiplied by the larger integral, yields the smaller integral.

American Polymer Standards Corporation [15] conducted molecular mass analysis using gel permeation chromatography (GPC) operating at 30 °C and using a Knauer Refractive Index detector. Samples were dissolved and analyzed in 1,1,1,6,6,6-hexafluoro-isopropanol (HFIP). Each sample was characterized five times yielding a standard uncertainty of 5% of the value (Table 3). The equipment was recalibrated between each data set using PA-6 standards with known molecular masses.

Thermal gravimetric studies (TGA) were conducted on a Thermal Analysis SDT 2960 simultaneous TGA/

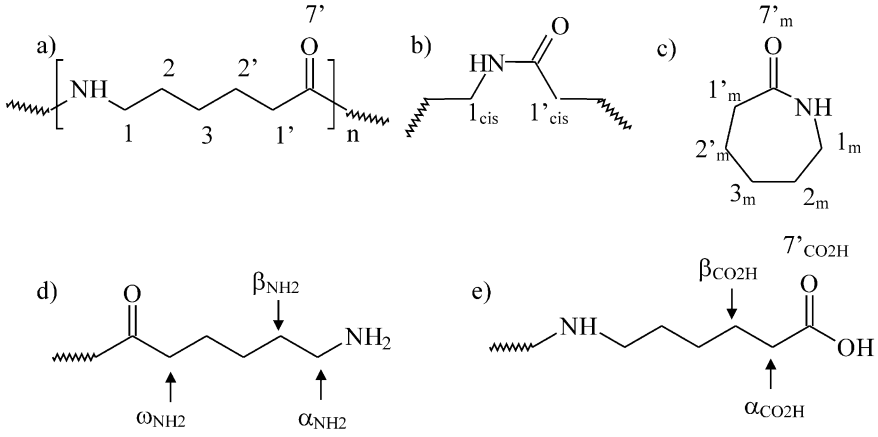

Fig. 3. Chemical structure and ^{13}C NMR peak nomenclature for (a) PA-6 (trans-amide linkage), (b) PA-6 (*cis*-amide linkage), c) ε-caprolactam, (d) PA-6 amine end-group and (e) PA-6 acid end-group.

Table 3
Composition data from GPC analysis of PA-6 and nanoPA-6 pellets and processed samples

Virgin PA-6	M_n (g/mol)	Nanocomposite PA-6	M_n (g/mol)
PA-6-e	16,050	MMT/PA-6-e	15,400
PA-6-i	17,850	MMT/PA-6-i	10,600
PA-6-i2	15,700	MMT/PA-6-i2	11,600

Analysis conducted by American Polymers Standards Corporation. Standard uncertainty is ±5% of the value (1 sigma).

DTA operating under 110 ml/min nitrogen flow; see Table 4 for experiment descriptions. All experiments were conducted in a nitrogen atmosphere and employed a heating rate of 40 °C/min; samples were cooled to room temperature at 15 °C/min in a nitrogen atmosphere. Each experiment was repeated four times resulting in an experimental uncertainty of ±0.2% mass fraction (1 sigma). The purpose of the TGA experiments 1–3 was to determine if volatiles were present in the polyamides prior to injection molding and after drying these polymers at various temperatures. The difference between the amount of volatiles lost during drying at 80, 120, and 180 °C and the amount of monomer these polymers contained prior to injection molding, as determined by NMR spectroscopy, is referred to as the "non-monomer" volatile content. It is assumed that no additional monomer formation occurred during drying since the drying temperatures are below the reported temperature for monomer formation.

Attenuated total reflectance infrared spectroscopy (ATR) was conducted on a Perkin Elmer 1760 FTIR using a Thunderdome single reflectance horizontal ATR cell equipped with a germanium crystal. One thousand transients were collected for each spectra and the resolution was 4 cm^{-1}.

4. Results and discussion

4.1. Polymer processing thermal stability

Using NMR, and GPC, we studied the thermal stability of PA-6 nanocomposites after processing at 300 °C. Solution ^{13}C NMR spectroscopy was used to determine (a) end-group and residual ε-caprolactam contents, (b) polymer number average molecular masses of as-received and processed virgin samples of both PA-6 (Figs. 4 and 5) and nanoPA-6 (Fig. 6), and (c) spectral

Table 4
Description of TGA experiments used to determine if volatiles, such as water, were present in the as-received PA-6 polymer and nanocomposite prior to processing

	Description	Reason
Experiment 1	Heat to 80 °C and hold for 4 h.	To determine volatiles lost from 80 °C drying process
Experiment 2	Heat to 120 °C and hold for 4 h.	To determine volatiles lost from 120 °C drying process
Experiment 3	Heat to 180 °C and hold for 4 h.	To determine volatiles lost from 180 °C drying process

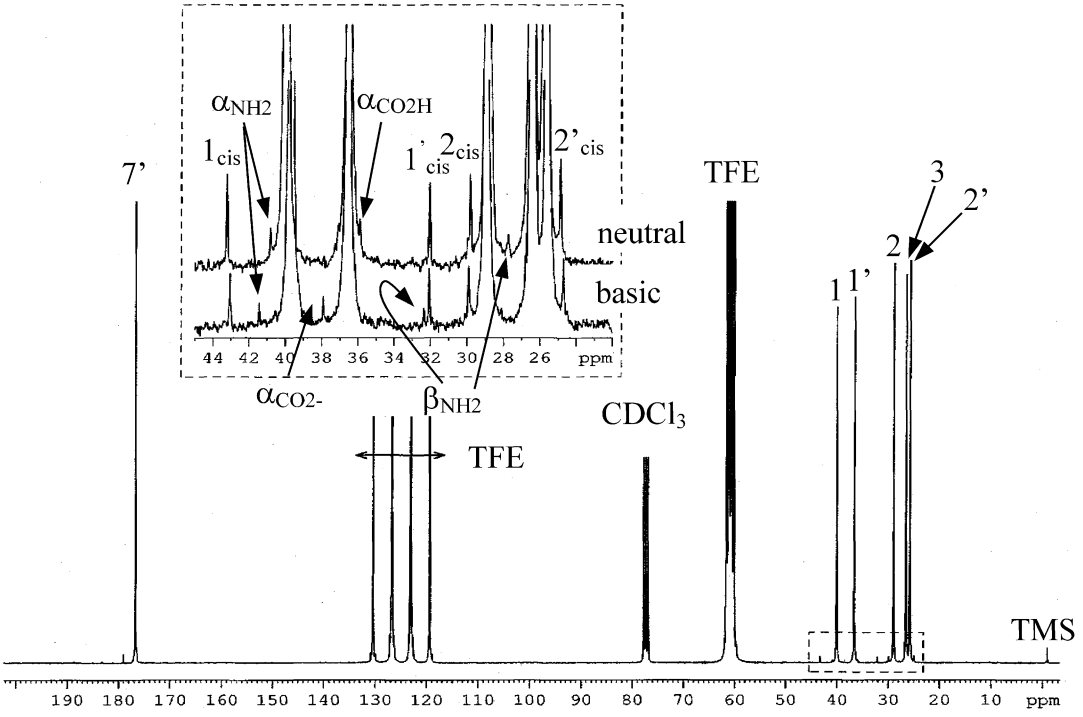

Fig. 4. Solution ^{13}C NMR spectra of PA-6-e taken in neutral NMR solvent. Expansion of PA-6-e spectra taken in the basic NMR solvent shows that the end-group peaks shift downfield, relative to their position in the neutral solvent, with little or no change in the other peak positions. Expanded spectra are plotted with same peak integrals. Slight peak broadening observed in the basic solvent caused the observed change in relative peak heights.

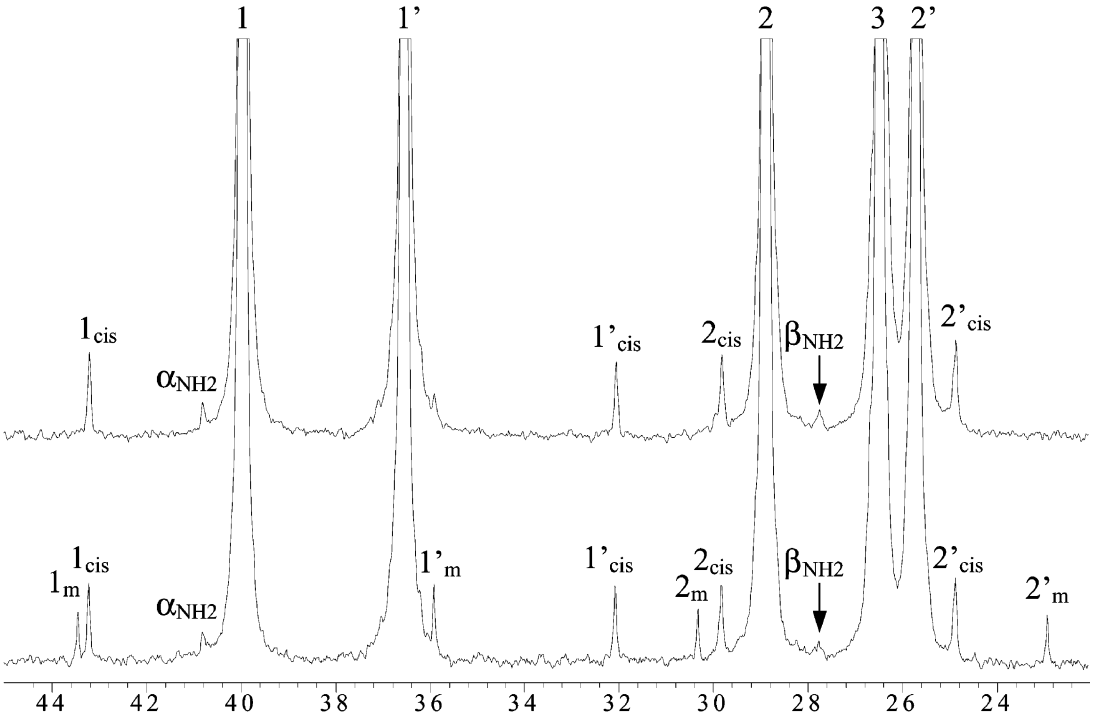

Fig. 5. Solution ^{13}C NMR spectra of PA-6-e (top) and PA-6-i (bottom) in neutral NMR solvent. Spectra are scaled based on integrals of *trans*-amide peaks. Polymer composition data is located in Table 2.

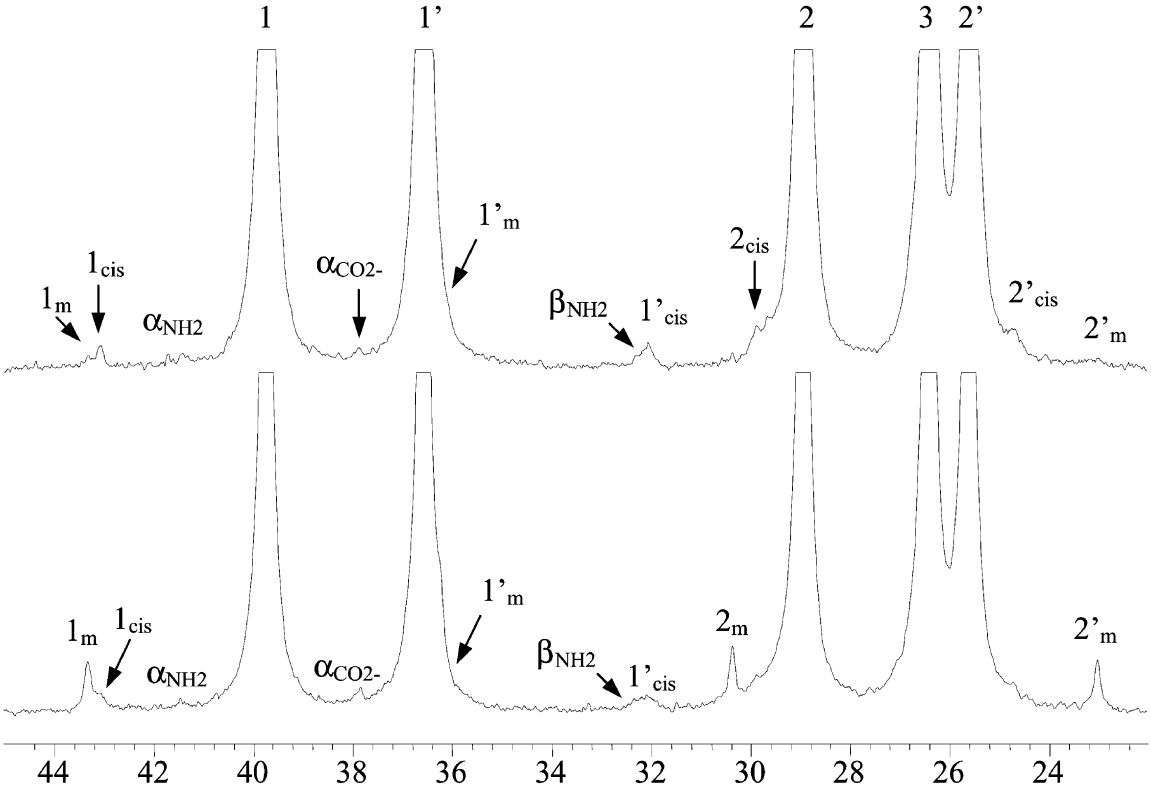

Fig. 6. Solution ^{13}C NMR spectra of as-received in situ polymerized MMT/PA-6-e (top) and after injection molding at 300 °C (bottom, MMT/PA-6-i), dissolved in basic NMR solvent. Spectra are scaled relative to the integrals of the *trans*-amide peaks. Polymer composition data is located in Table 2.

sensitivity to pH for nanoPA-6 dissolved in neutral or basic TFE-based NMR solvents [16,17][7]. Values in Table 2 are determined from characteristic peak integrals described in the experimental section and are provided in Table 2.

The solution ^{13}C NMR analysis of virgin PA-6 indicates that injection molding at 300 °C (12.5 min) does not lead to PA-6 degradation (Figs. 4 and 5). Within the NMR experimental uncertainty, virgin PA-6-e and-i compositions were nearly identical (Fig. 5 and Table 2). Virgin PA-6 number average molecular masses were near 13,000 g/mol, the fraction of total monomer repeat units having either acid or amine end-groups was 0.0083, and the ratio of acid to amine end-groups was equal; equal amounts of amine and acid end-groups are expected for a polymer that is synthesized via ring-opening polymerization.

Prior to processing nanoPA-6 pellets (MMT/PA-6-e) at 300 °C, the composition was similar to that of the virgin PA-6 pellets (13670 ± 1500 g/mol and end-group fraction was 0.0083 ± 0.0004); moreover, the ratio of acid to amine end-groups in each sample was equal (Fig. 5 and Table 2). However, after processing nanoPA-6 (regardless of drying conditions) number average molecular mass dropped nearly 40% to 7490 ± 630 g/mol (MMT/PA-6-i) and 8380 ± 1490 g/mol (MMT/PA-6-i2). Within the NMR uncertainty, the number average molecular mass for the two drying conditions is indistinguishable. Therefore, we conclude that extensive polymer degradation occurs during injection molding of nanoPA-6 at 300 °C, regardless of the drying conditions. The acid end-group fraction nearly doubled, 0.0151 (MMT/PA-6-i) and 0.0135% mass fraction (MMT/PA-6-i2), and the amine end-group fraction remained unchanged. Moreover, monomer fraction significantly increased from 0.0019 to approximately 0.04.

Molecular mass analysis by GPC also confirmed that nanoPA-6 pellets degraded during processing, regardless of drying conditions, whereas virgin PA-6 did not (Table 3). These results are in agreement with the NMR studies discussed above. However, the absolute values are slightly higher from GPC analysis. In most cases, within the combined experimental uncertainty of these techniques, the NMR values are approximately 80% of the GPC values. In addition, the GPC results indicate that the degree of degradation was less severe: approximately 30% reduction in molecular mass versus 40%. A possible explanation for these differences may be that the NMR analysis overestimates end-group content.

4.2. Polymer water content

Polyamides are notorious for containing a certain amount of equilibrium water and it is this water that can lead to PA-6 degradation if not removed prior to processing at elevated temperatures [5]. In the TGA, the as-received PA-6 polymer and nanocomposite were dried at 80, 120, and 180 °C in nitrogen, in order to mimic drying in a convection oven at these temperatures. The experiments are described in Table 4 and the results are provided in Table 5. These experiments showed that the as-received virgin PA-6 polymer and nanocomposite both contained volatiles that could not be removed at 80 °C drying. Increasing the drying temperature resulted in an increase in volatile loss. In contrast to PA-6-e, nanoPA-6 showed a greater mass loss was observed at 180 °C as compared to 120 °C drying. Subtracting the fraction of monomer content in these polymers, as determined by NMR spectroscopy, from the total volatiles lost at these different drying temperatures, such as shown in Table 4 for the 180 °C dried polymers, leaves the amount of non-monomer volatiles contained in these polymers. Presumably, these non-monomer volatiles are water. In this calculation we are assuming that no additional monomer formation occurred during drying since the drying temperatures are below the reported temperature for monomer formation [5]. Even though cyclic oligomers, if less than a few repeat units, are volatile at the processing conditions, these materials have not been pre-exposed to conditions that would have lead to the formation of cyclic oligomers [9,10], therefore were also not included in non-monomer volatile calculations. Therefore, we assume mass loss is due to monomer and water.

Virgin PA-6 and nanoPA-6 dried at 80 °C prior to processing contained water during processing (Table 4). The amount of water contained in the nanocomposite was higher than observed in virgin PA-6 and more difficult to remove as evidenced by the increase in water loss at 180 °C, as compared to 120 °C, for nanoPA-6. The difference in water content is attributed to the presence of MMT. Possible explanations are additional water bound to residual sodium ions on the MMT surface, water resulting from dehydroxylation of internal

[7] Changing the pH of the TFE/$CDCl_3$ solvent alters end-group chemical shift values without affecting other peaks in the solution ^{13}C NMR spectra [16,17]. The advantages of the basic NMR solvent are illustrated in Fig. 4; spectra of virgin PA-6 at 10% mass fraction concentration in neutral and basic solvent. In neutral solvent at 10% mass fraction polymer concentration, α_{NH2}, α_{CO2H}, and β_{NH2} peaks are overlapping with 1, 1′ and 2 peaks, respectively; thus integration of the end-group peaks is only reproducible to within ±30% of the average integral value. In the basic solution, these end-group peaks shift downfield and become baseline resolved and easily integrated to within ±5–10% of the average integral values. The pH value of nanoPA-6/basic NMR solvent solution was kept near 11. At pH values greater than 11 or less than 9, end-group peaks could not be resolved from larger polymer main chain peaks. PA-6-e composition was identical regardless of NMR solvent pH value (Figs. 4 and 5, and Table 2). No change in PA-6-e composition was observed over 1 week indicating that these solvents do not degrade PA-6.

Table 5
The amount of volatiles removed at various drying temperatures was determined using isothermal TGA for 4 h

As received pellets	% Mass loss determined by TGA[a]				
	Isothermal in N_2 for 4 h			% Monomer (not dried, determined by NMR)	% Non-monomer volatiles at 180 °C drying
	80 °C	120 °C	180 °C		
PA-6-e	0.0	0.67	0.65	0.0	0.65
MMT/PA-6-e	0.0	0.95	1.12	0.19	0.93

The amount of volatiles lost at 180 °C drying less the percent monomer, as determined by NMR of the as-received pellets, is the % non-monomer volatiles contained in these samples.

[a] Standard uncertainty of TGA mass loss percentages is ±0.2 mass% (1 sigma).

and edge hydroxyls in MMT, [18] and perhaps PA-6 near the clay surface has a larger infinity for water as a result of an altered amorphous domain structure.

The observation of volatiles that have been attributed to water may explain the observed degradation of the injection molded nanoPA-6, as compared to the as-received pellets (Table 2). However, removing more water by drying at 120 °C rather than 80 °C did not reduce the amount of polymer degradation. This may indicate that only a catalytic amount of water is needed for degradation to occur or that the amount of water only represents a portion of the water that the nanoPA-6 contains. We observed at higher drying temperatures, such as 300 °C, more volatiles were removed from MMT/PA-6-e; fraction of volatiles was 0.0398. However, it is not known how much of this fraction was water and how much is monomer since at 300 °C water can induce further monomer formation before volatilization.

4.3. Ammonium organic modifier thermal stability

IR spectroscopy of MMT/PA-6-i showed the presence of unsaturation groups (965 cm^{-1}) [19] that were not observed in virgin PA-6 or the unprocessed PA-6 nanocomposite (Fig. 7). VanderHart [4] has observed degradation of a quaternary alkyl ammonium bound to MMT in PA-6 after exposure to 240 °C during melt blending and extrusion and Vaia [20] has shown similar thermal instability of various alkyl ammonium organic modifiers. In the case of a primary ammonium, the degradation generates ammonia and an olefin (Fig. 8), which may explain the observed carbon–carbon double bond (unsaturation) by IR spectroscopy, and a proton possibly bound to the clay surface. In nanoPA-6, the ammonium lauric acid modifier is covalently linked to the PA-6 [21,22] although not all PA-6 chains are linked. NanoPA-6 end-groups are thus amine, acid, and ammonium, therefore, the ammonium degradation results in some PA-6 chains with an unsaturation end-group. This may explain why the amine end-group content was less than the acid end-group content in MMT/PA-6-i.

4.4. Polymer degradation pathways

We propose a possible degradation mechanism, based on TGA, GPC, NMR and IR results. Water from MMT clay (bound or from dehydroxylation) and absorbed by PA-6, causes hydrolysis of PA-6 peptide linkages (Fig. 1B). This significantly reduces PA-6 number average molecular mass and increases acid and amine end-group concentration in processed MMT/PA-6 nanocomposites. In this scheme, amine end-group concentration can remain static because a portion of the

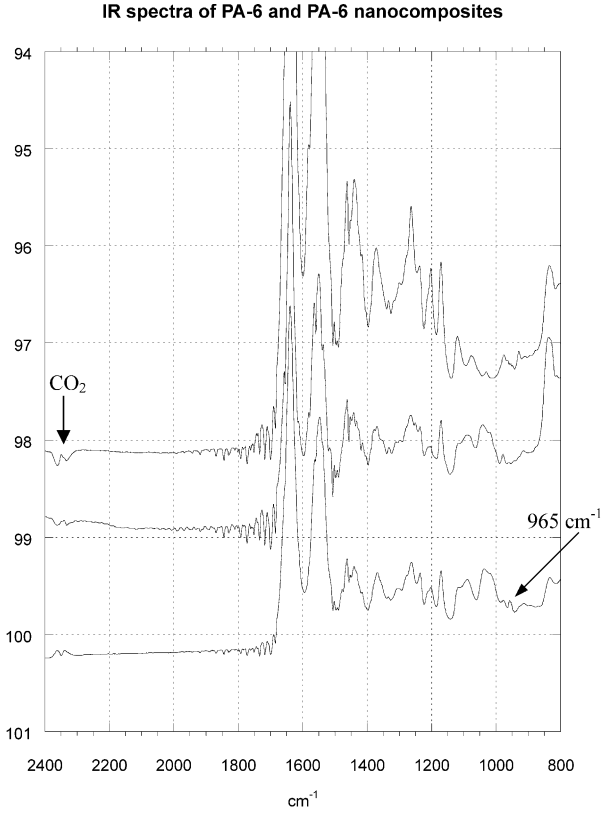

Fig. 7. IR spectra of pure PA-6 (top), as-received nanoPA-6 pellets (middle), and nanoPA-6 after injection molding at 300 °C (bottom). No nitrile groups were observed near 2245 cm^{-1}. A vinyl peak observed only in the injection molded nanocomposite at 965 cm^{-1} indicates the presence of unsaturated end-groups, which was not observed in the other materials.

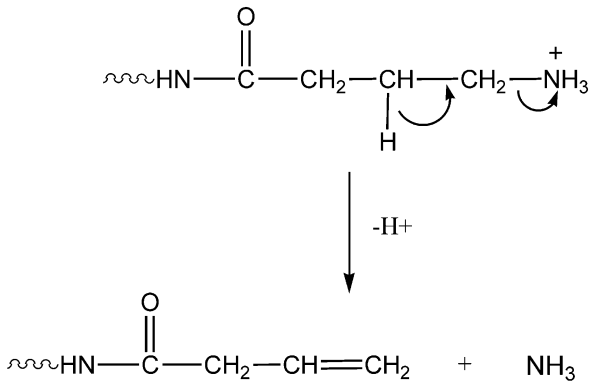

Fig. 8. Degradation of ammonium end-group begins near 200 °C and generates a free amine or ammonium (not shown) group and an unsaturation end-group. An unsaturation group was detected by IR spectroscopy implying that this elimination may have occurred.

amine end-groups were ammonium end-groups that degraded during processing into terminal unsaturations (terminal unsaturations were observed by IR and not by NMR, Fig. 7), as shown in Fig. 8.

The degradation of a mono-alkylated ammonium group generates ammonia (due to loss of the alkyl group) that could bind to MMT, then degrade leaving acidic clay and free amine, or could volatilize. The free amine is a good nucleophile and could also fracture peptide linkages, resulting in a nitrile or methyl end-group (see degradation products of amide end-group in Fig. 1A). Neither end-group was observed by NMR or IR spectroscopy, therefore we concluded that within the sensitivity of these techniques, PA-6 peptide scission in nanoPA-6 does not result from this pathway.

Another possible degradation mechanism, which may not be independent of the previous pathway, is MMT catalyzed PA-6 degradation. The ability of clay minerals to catalyze peptide formation and degradation from and to amino acids was investigated by numerous researchers over the past 40–50 years; for example Budjak et al. [23] and Lahav et al. [24] In these studies, the catalytic activity was attributed to the cationic clay treatment (Cu^{2+} and Ca^{2+}[23], and Na^{+}[24]). Since complete organic exchange of MMT is never achieved there is still residual sodium, therefore this may be a concern [25].

Prior to polymer and clay mixing, the clay is treated (ion exchanged) with an organic modifier to increase the gallery spacing and to improve polymer/clay interactions. Full exchange of all sodium cations to organic modifier does not occur. In fact, it is possible that up to 10% of the cation exchange capacity value of sodium cation is remaining in the nanoPA-6 investigated. These unexchanged sodium cations may have been involved in PA-6 degradation, perhaps by binding with the peptide linkages of PA-6 with the result that there is hydrolytic peptide scission in the presence of water.

Other portions of MMT may catalyze PA-6 degradation. For example, Stucki has shown that the structural elements of MMT, such as Fe^{2+} and Fe^{3+}, catalyzed pesticide transformations [26]. The pesticides were small moieties that did not structurally resemble PA-6 or the functionality contained within. However, the pathway is that of a Lewis base and PA-6 is susceptible to base attack, especially at elevated temperatures.

5. Conclusions

The results of this investigation have led us to the following observations and conclusions about the thermal stability of PA-6 and nanoPA-6 during processing at 300 °C and one's ability to dry these materials prior to processing.

1. NanoPA-6 significantly degraded during processing at 300 °C. Within experimental uncertainty, drying at 120 °C rather than 80 °C prior to processing had little effect on the degree of degradation. Virgin PA-6 did not degrade under identical processing conditions.
2. NanoPA-6 thermal decomposition may have resulted from hydrolytic peptide scission. The catalytic activity of MMT was not studied here, however, based on previous research, MMT could be involved in PA-6 thermal degradation.
3. Heating at 120 °C for 4 h thoroughly dried virgin PA-6; 80 C drying resulted in no water loss. The amount of volatile water in nanoPA-6 was greater than observed in virgin PA-6. Longer drying times and higher temperatures resulted in drier nanoPA-6.
4. We propose that MMT and water are responsible for the degradation of nanoPA-6.
5. When PA-6-e polymer was processed at 300 °C some water was present, however, little degradation was observed. This means that: (a) water itself may not be sufficient to cause degradation (b) water escapes from PA-6 faster than from the nanocomposite (c) clay and water are a special catalyst combination and/or d) clay is a source of high-temperature reactive water or hydroxyls.

References

[1] Kojima Y, Usuki A, Kawasumi M, Okada A, Fukushima Y, Kurachi T, et al. Mechanical properties of Nylon 6-clay hybrids. J Mater Res 1993;8:1185.
[2] Kojima Y, Usuki A, Kawasumi M, Okada A, Kurachi T, Kamigato O. One-pot synthesis of Nylon 6-clay hybrids. J Polym Sci Polym Chem 1993;31:1755.
[3] Pinnavaia TJ, Beall, GW. In: Pinnavaia, TJ, editor. Polymer-clay nanocomposites. John Wiley and Sons; 2000.
[4] VanderHart DL, Asano A, Gilman JW. Solid state NMR inves-

tigation of paramagnetic Nylon-6 clay nanocomposites. Macromolecules 2001;34(12):3819.
[5] Levchik SV, Weil ED, Lewin M. Review: thermal decomposition of aliphatic nylons. Polym Int 1999;48:1.
[6] Dussel H-J, Rosen H, Hummel DO. Makromol Chem 1976; 177:13.
[7] Ohatani H, Nagaya I, Sugimura Y, Tsuge S. J Anal Appl Pyrol 1982;4:117.
[8] Levchik SV, Costa L, Camino G. Effect of the fire-retardant, ammonium polyphosphate, on the thermal decomposition of aliphatic polyamides: part II—polyamide 6. Polym Degrad Stab 1992;36:229.
[9] Luderwald I, Mertz F, Rothe M. Agnew Macromol Chem 1978; 67:193.
[10] Ballestreti A, Garozzo D, Giufrida M, Impallomenti G, Montaudo G. Polym Degrad Stab 1988;23:25.
[11] Hornsby PR, Wang J, Rothon R, Jackson G, Wilkinson G, Cossick K. Thermal decomposition behavior of polyamide fire-retardant compositions containing magnesium hydroxide filler. Polym Degrad Stab 1996;51:235.
[12] Ube Industries, Ltd. (Japan).
[13] Thermoplastics Troubleshooting Guide, Ashland Chemical Company; 1997.
[14] pH values were determined on litmus paper dampened with water.
[15] American Polymer Standards Corporation, 8680 Tyler Boulevard, Mentor, OH, 44060, (440)-255–2211.
[16] Davis RD, Steadman SJ, Jarrett WL, Mathias LJ. Solution ^{13}C NMR characterization of Nylon 66: quantitation of *cis*-amide conformers, acid and amine end-groups, and cyclic unimers. Macromolecules 2000;33(19):7088–92.
[17] Davis RD, Jarrett WL, Mathias LJ. Solution ^{13}C NMR spectroscopy of polyamide homopolymers (Nylons 6, 11, 12, 66, 69, 610, 612) and several commercial copolymers. Polymer 2001;42:2621–6.
[18] Stucki JW. Private communication.
[19] Kamerbeck G, Kroesw H, Grotle W. Soc Chem Monogr No 1961;13:357.
[20] Xie W, Gao Z, Pan WP, Hunter D, Singh A, Vaia R. Thermal degradation chemistry of alkyl quanternary ammonium montmorillonite. Chem Mater 2001;13:2979.
[21] Kurachi T, Okada A, Nomura T, Nishio T, Saegusa, S, Deguchi R. Nylon 6-clay hybrid—synthesis, properties and application to automotive timing belt cover. SAE Tech. Paper Series, Patent # 910584, 1991.
[22] Davis RD. Solution and solid state nuclear magnetic resonance spectroscopy of polyamides and crosslinked polyacrylates. Dissertation, School of Polym. Sci. and Eng, Univ. Southern. Miss., 2001.
[23] Budjak J, Sloriarikova H, Texler N, Schwendiger M, Rode BM. On the possible role of montmorillonites in prebiotic peptide formation. Monatshefte fur Chemie 1994;125:1033.
[24] Lahav N, White D, Chang S. Peptide formation in the prebiotic era: thermal condensation of glycine in fluctuating clay environments. Science 1978;201:67.
[25] Southern Clay Websites.
[26] Cervini-Silva J, Wu J, Stucki JW, Larson RA. Environ Sci Tech 2001;35:805.